Supporting Information

A fluorinated bifunctional additive achieving stable electrode/electrolyte interfaces for high-voltage lithium-metal batteries

Lei Zeng,[a,b] *Lu Gao,*[b] *Ting Ou,*[c] *Yufan Xin,*[b] *Junliang Du,*[a,b] *Mengqi Wang,*[a,b] *Yanshuang Meng,*[a,*]

Xiaopeng Pei,[b,*] *and Ying Tan* [b*]

[a] School of Materials Science and Engineering, Lanzhou University of Technology, Lanzhou 730050, China

[b] Wenzhou Institute, University of Chinese Academy of Sciences, Wenzhou 325000, China

[c] Institute of Theoretical and Computational Chemistry, Shaanxi Key Laboratory of Catalysis, School of Chemical & Environment Science, Shaanxi University of Technology, Hanzhong, 723001, China

* Corresponding authors:

E-mail: mengyanshuang@163.com (Y. Meng); peixiaopeng@ucas.ac.cn (X. Pei); tanying@ucas.ac.cn (Y. Tan)

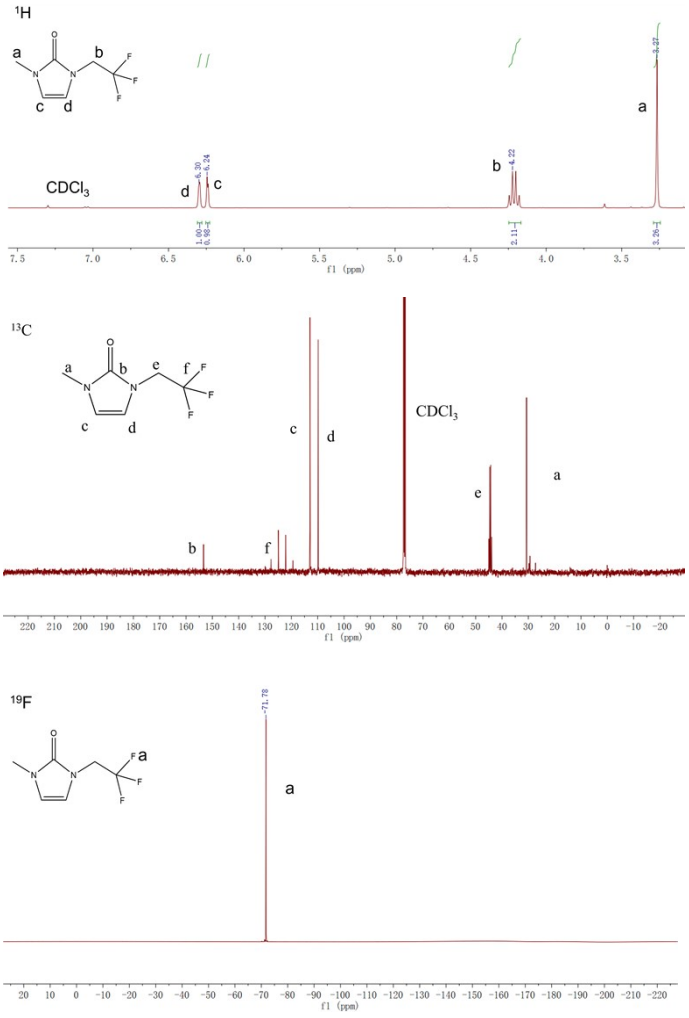

Fig. S1. ^{1}H, ^{13}C and ^{19}F NMR spectra of M-3FEn-IO in $CDCl_3$.

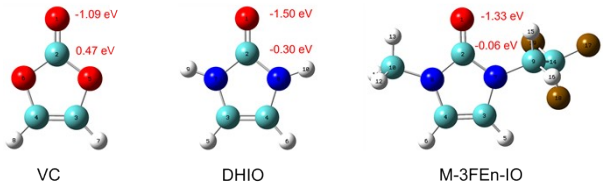

Fig. S2. The average electrostatic potential of the surface near the atoms in the molecule.

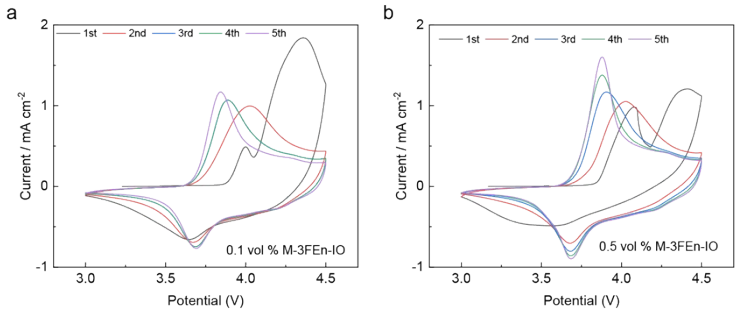

Fig. S3. CV of the first five circles of Li || NCM622 cells with electrolytes containing (a) 0.1 and (b) 0.5 vol % M-3FEn-IO in the voltage range of 3 - 4.5 V at a scan rate of 0.5 mV s^{-1}.

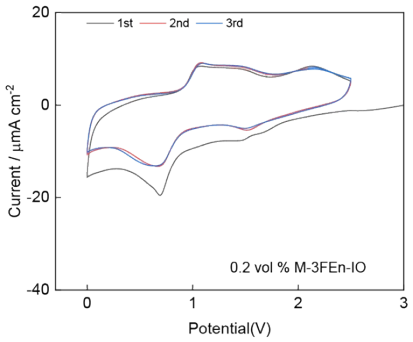

Fig. S4. CV curves of Li || SS cells 0.2 vol % M-3FEn-IO, at the first three cycles in the 0 - 2.5 V voltage range at a scan rate of 0.5 mV s^{-1}.

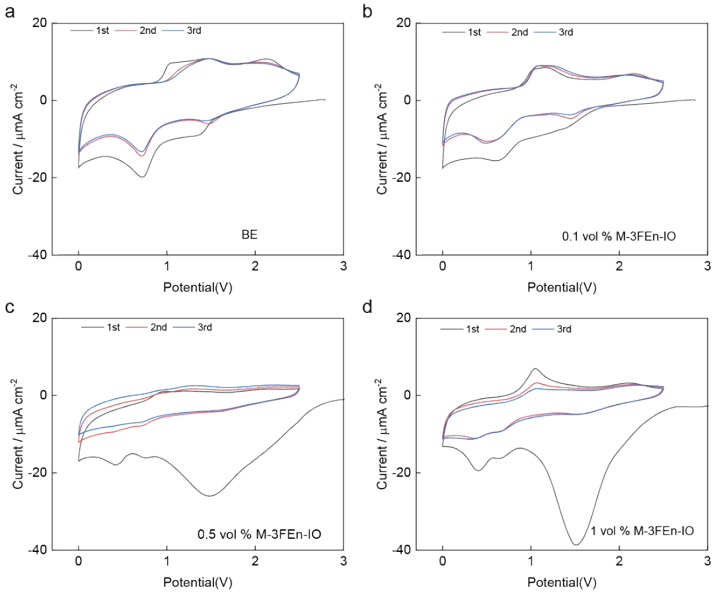

Fig. S5. CV curves of Li || SS cells with different electrolytes at the first three cycles in the 0 - 2.5 V voltage range at a scan rate of 0.5 mV s^{-1}.

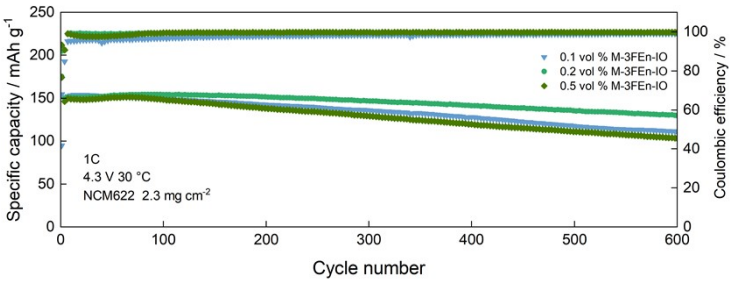

Fig. S6. Capacity retention of Li || NCM622 batteries with the electrolytes containing varying additive concentrations. The cells were initially activated at 0.2 C and then cycled at 1 C with a cut-off voltage of 4.3 V at 30 °C.

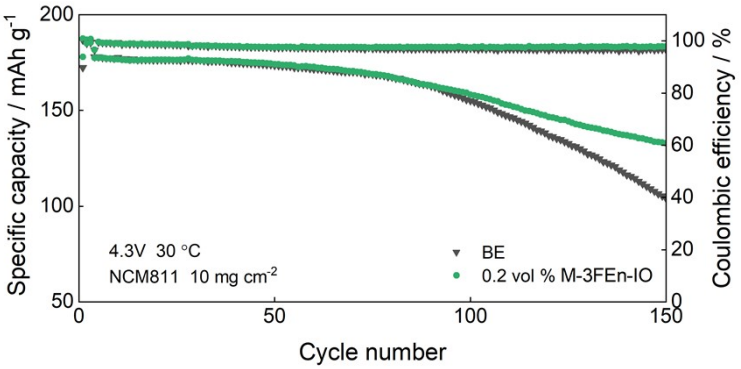

Fig. S7. Capacity retention of Li || NCM622 batteries with the BE and electrolytes containing varying additive concentrations. The cells were initially activated at 0.2 C and then cycled at 1 C with a cut-off voltage of 4.3 V at 30 °C.

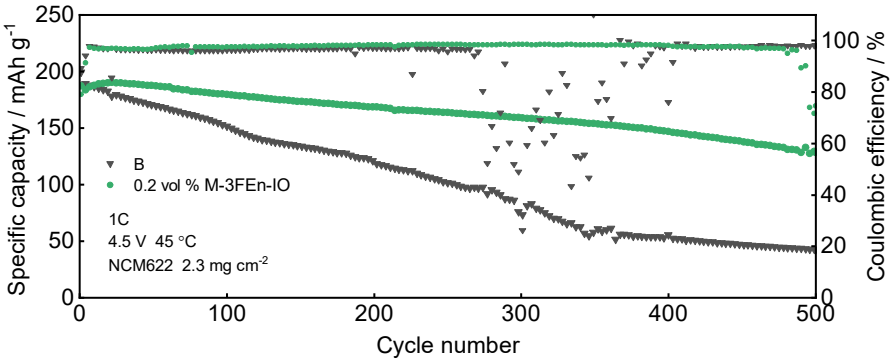

Fig. S8. Cycling performance of the Li || NCM622 battery after activation at 0.2 C and 45 °C, followed by 1 C cycling with a 4.5 V cut-off. Capacity retention is shown over cycle number.

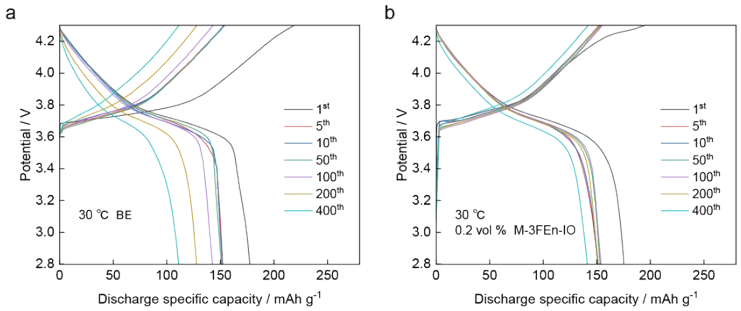

Fig. S9. The electrochemical cycling performance of a Li || NCM622 battery was evaluated at 1 C after initial activation at 0.2 C and at a temperature of 30 ℃. The charge and discharge curves of the Li || NCM622 battery were measured while cycling with both BE (a) and (b) electrolyte containing 0.2 vol % M-3FEn-IO.

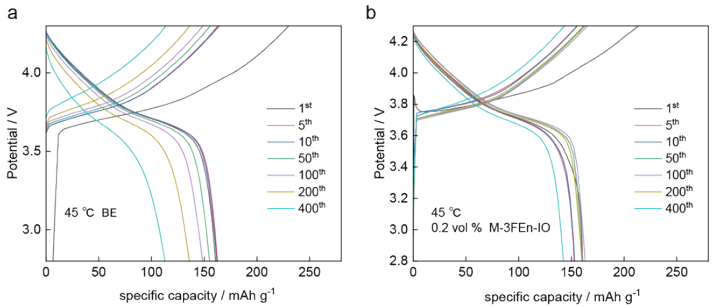

Fig. S10. The electrochemical cycling performance of a Li || NCM622 battery was evaluated at 1 C after initial activation at 0.2 C and at a temperature of 45 ℃. The charge and discharge curves of the Li || NCM622 battery were measured while cycling with both (a) BE and (b) electrolyte containing 0.2 vol % M-3FEn-IO.

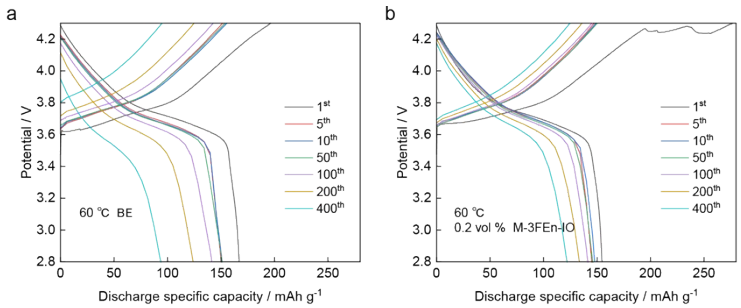

Fig. S11. The electrochemical cycling performance of a Li || NCM622 battery was evaluated at 2 C after initial activation at 0.2 C and at a temperature of 60 ℃. The charge and discharge curves of the Li || NCM622 battery were measured while cycling with both (a) BE and (b) electrolyte containing 0.2 vol % M-3FEn-IO.

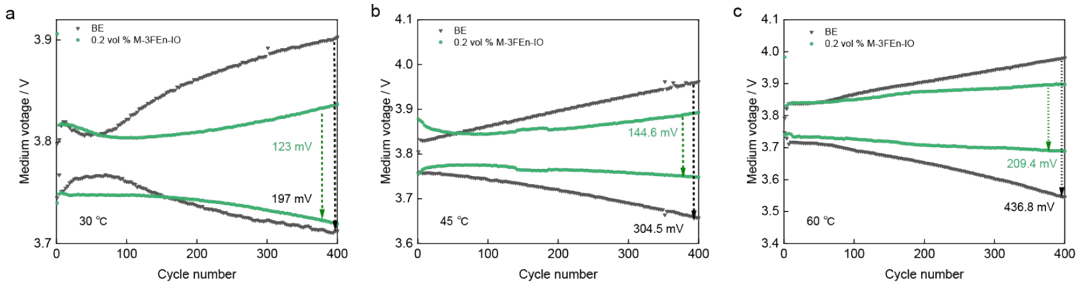

Fig. S12. Evolution of charge and discharge medium voltages during cycling for the BE and the battery containing 0.2 vol % electrolyte additive. After initial activation at 0.2 C, the cells were tested under elevated temperatures of (a) 30 ℃ and (b) 45 ℃ at a current rate of 1 C, and (c) 60 ℃ at a current rate of 2 C.

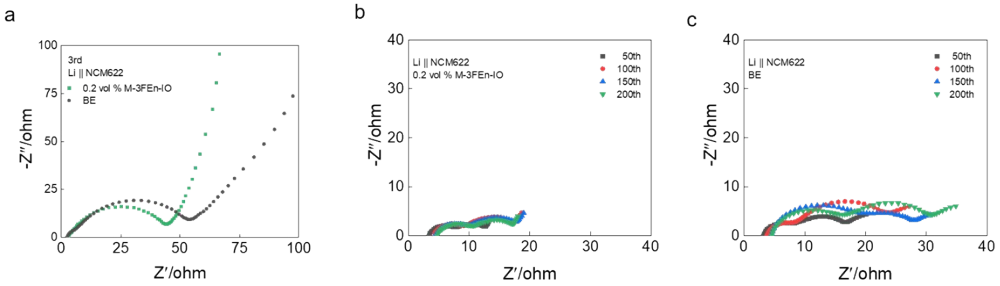

Fig. S13. EIS spectra of Li || NCM622 cells employing the BE and the electrolyte modified with 0.2 vol % M-3FEn-IO additive after the 3rd, 50th, 100th, 150th and 200th charge-discharge cycles.

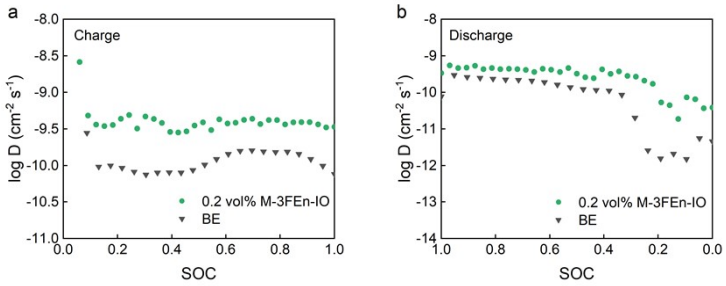

Fig. S14. The Li^+ diffusion coefficient was derived from the charge-discharge profiles of the activated Li||NCM622 cell.

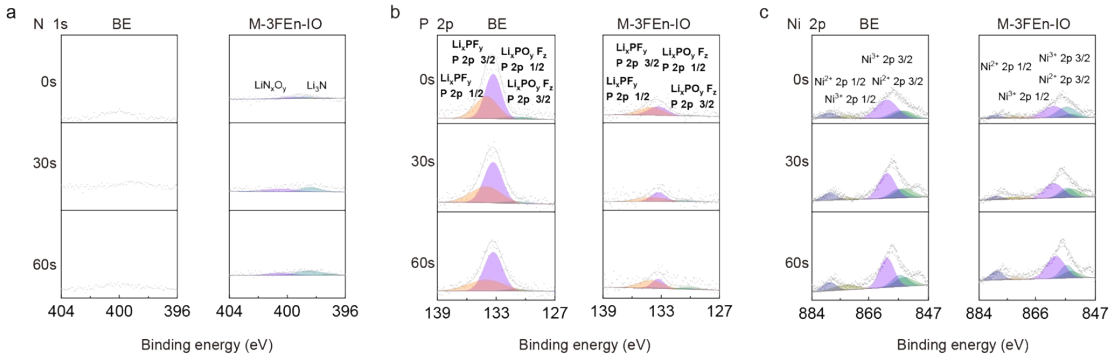

Fig. S15. XPS spectra of (a) N 1s, (b) P 2p and (c) Ni 2p for the cycled NCM622 cathode electrode with BE and 0.2 vol % M-3FEn-IO containing electrolyte.

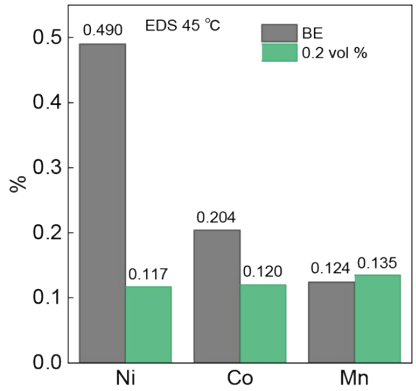

Fig. S16. EDS spot scanning of Ni, Co, and Mn elements on the LMA surface after 100 cycles of Li || NCM622 batteries with different electrolytes at 45 ℃.

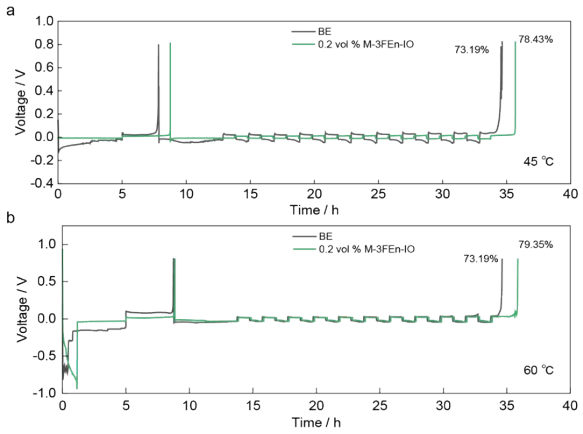

Fig. S17. Evaluation of the CE of the Li || Cu battery using different electrolytes via the Aurbach's method at (a) 45 °C and (b) 60 ℃.

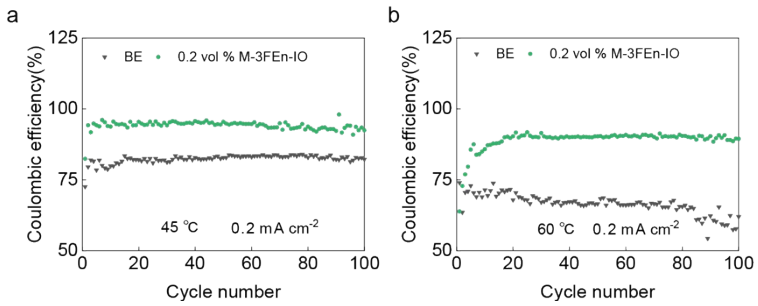

Fig. S18. The CE of the Li || Cu battery using BE and the electrolyte containing 0.2 vol % M-3FEn-IO at 0.2 mA cm^{-2}, at (a) 45 °C and (b) 60 °C.

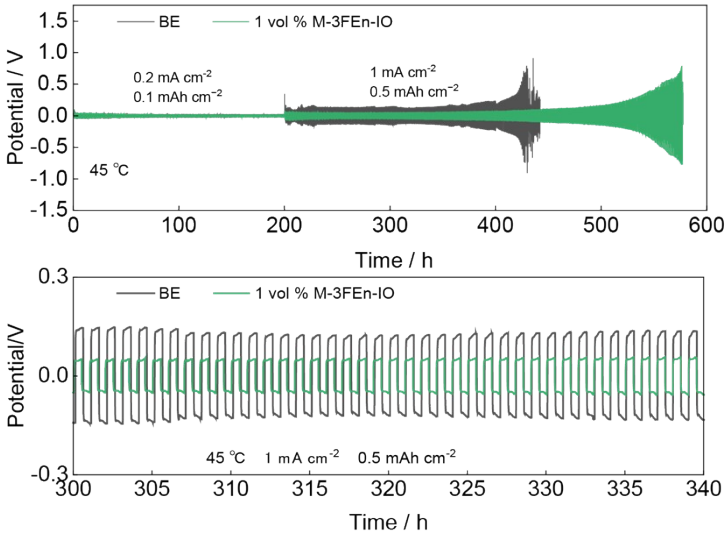

Fig. S19. Long-term cycling performance of a Li || Li battery was evaluated at 45 °C using an electrolyte containing BE and 1 vol % M-3FEn-IO at current density of 0.2 mA cm^{-2} and 0.1 mAh cm^{-2} for the initial two hundred cycles, followed by a higher current density of 1 mA cm^{-2} and 0.5 mAh cm^{-2}.

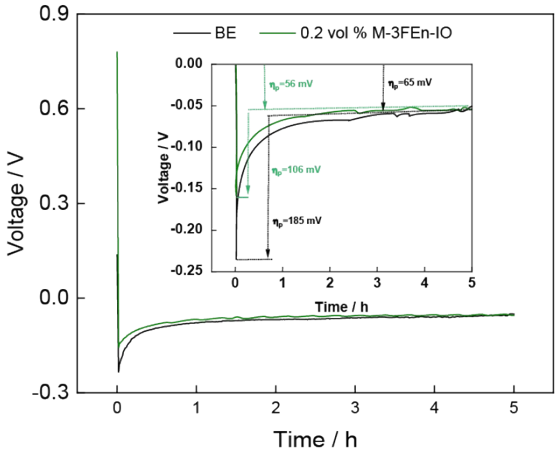

Fig. S20. Voltage curves during the initial discharge process of the Li || Cu battery using BE and the electrolyte containing 0.2 vol % M-3FEn-IO.

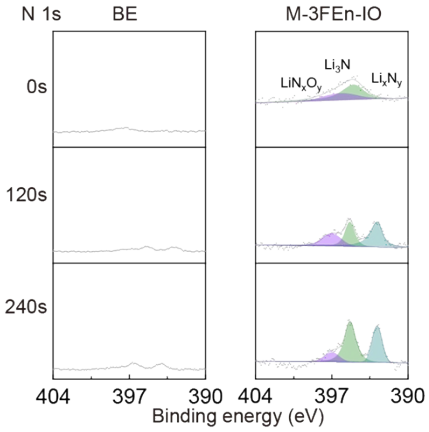

Fig. S21. XPS spectra of N 1s of the cycled Li anode electrode using the BE and electrolyte containing 1 vol % M-3FEn-IO.